

CONF-9010299--1

UCRL-JC-105042
PREPRINT

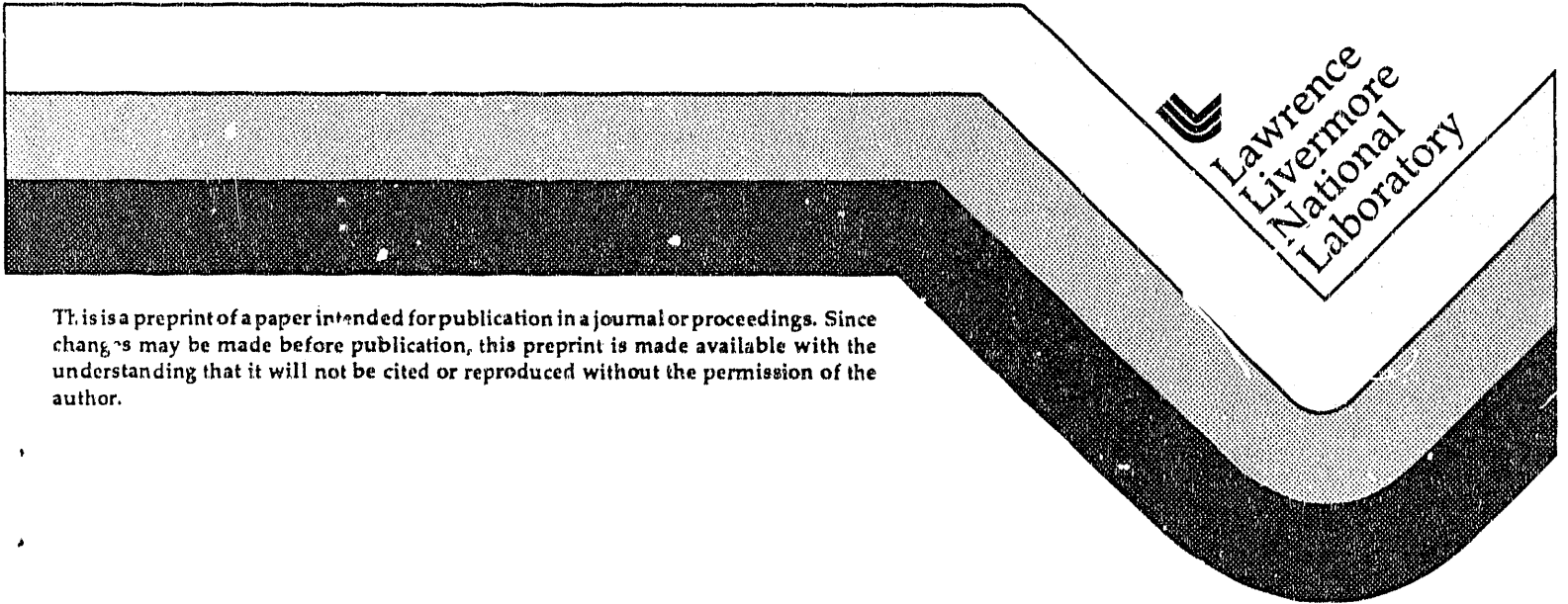
Received
JAN 16 1991

Fission Decay in Intermediate Heavy Ion Reactions

Harold C. Britt
E Division/Physics Department

This paper was prepared for submittal to the Proceedings of the International Symposium on Heavy Ion Physics and Its Applications Lanzhou, Peoples Republic of China 7-13 October 1990

October 3, 1990



This is a preprint of a paper intended for publication in a journal or proceedings. Since changes may be made before publication, this preprint is made available with the understanding that it will not be cited or reproduced without the permission of the author.

MASTER

DISCLAIMER

This document was prepared as an account of work sponsored by an agency of the United States Government. Neither the United States Government nor the University of California nor any of their employees, makes any warranty, express or implied, or assumes any legal liability or responsibility for the accuracy, completeness, or usefulness of any information, apparatus, product, or process disclosed, or represents that its use would not infringe privately owned rights. Reference herein to any specific commercial products, process, or service by trade name, trademark, manufacturer, or otherwise, does not necessarily constitute or imply its endorsement, recommendation, or favoring by the United States Government or the University of California. The views and opinions of authors expressed herein do not necessarily state or reflect those of the United States Government or the University of California, and shall not be used for advertising or product endorsement purposes.

FISSION DECAY IN INTERMEDIATE HEAVY ION REACTIONS

HAROLD C. BRITT
Lawrence Livermore National Laboratory
E Division/Physics Department
P.O. Box 808, Mail Code L-289
Livermore, CA 94550

UCRL-JC--105042

DE91 006255

ABSTRACT

Results are presented on cross sections, parallel and perpendicular momentum transfers, charge loss and velocity systematics for fission following reactions of Fe and Nb projectiles at 50-100 MeV/A on targets of Ta, Au, and Th. The results at 100 MeV/A are compared to a detailed multistage deexcitation model. The initial collision is modeled with an intranuclear cascade. The resultant excited target residues then undergo a fast preequilibrium decay stage followed by a statistical decay involving nucleon evaporation and fission. Results from this modeling are in reasonable agreement with experimental data.

I. INTRODUCTION

The fission of a heavy nuclear system provides an excellent tool for studying the latter stages of a complex, high energy nuclear reaction. Coulomb energy systematics give a clear indication for the binary fission process while fragment angular correlations and mass and energy distributions can be used to estimate average quantities such as linear momentum transfer and the mean mass and excitation energy for the fissioning system. A comprehensive review of fission utilized as a filter for studying reaction mechanisms has recently been published by Viola [1].

In a recent experimental program at the LBL BeValac our group [2] has developed a new logarithmic multidetector system [3] capable of measuring charges and energies of particles emitted in medium energy heavy ion reactions. This detector system shown schematically

in Fig. 1 has a very broad acceptance in charge, velocity, and angle making possible a full inclusive characterization of the reactions and a variety of correlation measurements. In this report the systematics of the fission reactions are briefly presented. A more comprehensive presentation of this data is presented elsewhere [4]. Results are presented for 50-100 MeV/A projectiles of Fe and Nb bombarding targets of Ta, Au and Th. In an attempt to characterize these results a simple model based on previous knowledge of medium energy reactions and on current theories of fission has been developed. This model described in more detail elsewhere [5] does a reasonable job of reproducing the experimental results without the necessity of introducing any new physical constructs that are particular to this new region of projectile mass and energy.

II. EXPERIMENTAL DATA

For the data presented in this report a determination of the velocity and charge, Z , of each detected fragment was obtained from the signals in the low pressure proportional counter and the two multiwire proportional counters (See Fig. 1). Figure 2 shows a typical spectrum where the separation between fission fragments, heavy residues and intermediate mass fragments is clearly evident.

Figure 3 shows a Z_1 - Z_2 contour distribution for binary events. The data separate into two distinct regions. The region closest to the origin contains events in which one of the two fragments may be in the fission-mass range but where the sum $Z_1 + Z_2$ is generally less than half Z_{targ} . This implies that the breakup of the residual system is not binary and that other fragments have been emitted outside the acceptance of the detector array. The other region consists entirely of events in which the sum $Z_1 + Z_2$ is close to but less than Z_{targ} and each fragment has a charge greater than about 25. In addition to a symmetric binary charge distribution, fragments in this region have a relative velocity distribution consistent with low energy fission systematics.

Figure 4 shows measured mean values for the parallel and perpendicular momentum transfers in these reactions. The parallel

momentum transfer correlates with the fissility of the target as predicted in the model described below. The perpendicular momentum transfer is primarily dependent on the projectile mass. The energy dependences are consistent with a simple picture where fission for a given target residue always occurs at about the same excitation energy.

In Fig. 5 data for the system Fe + Th is compared to existing data taken from Ref. 6. The mean values for the linear momentum transfer per nucleon are significantly lower than in previous studies utilizing projectiles of mass 1-20. This result is qualitatively consistent with the concept of fission as a collective process which samples only the final fully equilibrated stages of target residue decays. At high excitation energies the target residue becomes increasingly less fissionable because the nucleus remaining after the fast preequilibrium processes becomes lighter and less fissile. This feature is also reproduced in our simple model.

In Figure 6 we show a correlation between the parallel momentum transfer per nucleon and the measured parallel momentum per nucleon. The results give further validity to the technique of using folding angle distributions to estimate parallel momentum transfers as has been used in previous studies [1,6].

III. THE FISSION MODEL

In heavy ion reactions at energies of 100 MeV/A and above, Intranuclear Cascade models (INC) [7,8] have been successful in predicting the properties of the prompt emission associated with the initial direct cascade. However, little has been done to model in detail the decay of the highly excited residues which are produced. These residues have many properties in common with the compound systems produced in heavy ion reactions at much lower energies where more extensive experimental and theoretical studies have been performed.

We now present a reaction model which involves an INC calculation using the Yariv-Franekel code [7,8] followed by an empirically modelled pre-equilibrium fast cascade leading into a

statistical decay modelled by the code PACE [9]. The primary objective of this effort was to see if such an approach could quantitatively describe the fission decays which generally occur at the end of the cascade. If this technique can be further developed and tested then it may be possible to use fission to study the Z , mass and angular momentum distributions of target residues created in high energy heavy ion reactions.

In Figs. 7,8 we show the correlations between impact parameter, parallel momentum transfer, spin and mass of the target residual from the INC calculations. It is seen that there is a strong correlation between parallel momentum and excitation energy.

The model is described in detail elsewhere [5]. Below we give only the major characteristics of the calculations. Before entering a statistical decay model, nuclei produced by the intranuclear cascade calculation having excitation energies between 300 and 1000 MeV first undergo a fast nucleon cascade. For modeling the deexcitation in the 300 to 1000 MeV region we employ a fast nucleon emission mechanism. In this decay the choice between proton or neutron emission is based on the relative number of neutrons and protons in the excited nucleus. The particle energy spectrum is taken as a Maxwellian with a slope parameter of 15 MeV. The angular momentum removed by these particles is assumed to be $2/3$ of the maximum allowed value. Then products remaining with $E_x < 300$ MeV were analyzed using the PACE statistical model code. This code is described elsewhere [9]. We have modified the code to enable us to follow the deexcitation of any resultant fission products. From 300 MeV to 150 MeV of excitation energy the system is allowed to statistically evaporate particles, and the angular momentum is explicitly followed. In this excitation energy range fission is not allowed to compete as a decay channel. This choice is made as a simple approximation for the dissipative and flow dynamic effects that impose minimum times for fission to become a viable decay channel [10,11]. At excitation energies below 150 MeV, fission is allowed as a decay channel in PACE with the relative level density parameters chosen to give $a_f/a_n = 1.01$. The value of a_f/a_n and the

cutoff energy for fission were adjusted to give the best representation of previous proton and light heavy ion data [12,13]. Changes in the values of these parameters tend to proportionally scale all of the calculated cross sections. Thus, our model has effectively two adjustable parameters that were determined by a fit to the data in Refs. 12 and 13 and then held fixed for all subsequent calculations. These parameters are also a reasonable approximation of those that reproduce the integral fission cross sections that were calculated using the full flow dynamics consideration in the decay of Erbium isotopes [11].

IV. COMPARISONS WITH EXPERIMENT

The model has been used to calculate the fission yield observables in the 100 MeV/A data. The approach we have used is to apply an acceptance filter that includes the experimental geometries and efficiencies to the calculated quantities. The filtered calculations can then be directly compared with the experimental observables. Extensive Monte Carlo simulations were performed in order to find out which quantities have the strongest influence on the acceptance. Our simulations showed that only the parallel momentum and the scattering angle of the fissioning nucleus significantly affect the acceptance. Figure 9 shows the calculated and experimental differential cross sections as a function of parallel momentum for the four cases studied. Very good agreement is obtained for three of the four cases. For the Fe + Ta case, the experimental results are systematically above the calculated values. The differential shape is in reasonable agreement with the data but the yield is ≈ 5 times larger than the model prediction. This is the least fissile target and the experimental and theoretical statistics are the most limited. Figure 10 shows the calculated and observed fission laboratory angular distributions. As with the differential cross sections the agreement is excellent for the heavier targets. In the case of Ta, the discrepancy in absolute cross sections is again apparent - the shape is reproduced well but the absolute magnitude is substantially larger than calculated. For all cases, the theoretical angular distributions were calculated on the

assumption that fission occurs isotopically in the frame of the fissioning nucleus. The good agreement with experiment implies that the angular momenta of the fissioning systems are small and/or randomly oriented. Figure 11 shows the comparison of calculated and experimental mean values for ΔZ where the total Z of the two final fission fragments are compared to the Z of the target. Both the experimental and theoretical distributions peak near the target Z but the calculations give a considerably narrower peak. This difference results in the discrepancy observed in fig 11 which could be due to one or any combination of several effects that are difficult to differentiate at this point. First, the Z distribution coming from the initial INC calculations and remaining after the fast cascade may be too narrow. There is some indication of a similar effect in the comparison of measured isotopic residue distributions with INC calculations from the reaction $\text{Ne} + \text{Au}$ at 8 GeV [14]. In this case the INC calculation gives a distribution which is too broad in neutron number and again a relatively sharp distribution in atomic number. A second possibility is that the angular momenta calculated for large ΔZ residuals are too low for fission to compete in the deexcitation cascade. This could be due to the lack of collective effects in the intranuclear cascade calculation. The discrepancy could also be due to the empirical fast cascade taking away too much angular momentum.

V. SUMMARY

We have presented data on fission from bombardments of heavy targets by heavy mass intermediate energy projectiles and an attempt at a complete model to describe the formation and subsequent decay (including fission) of target residues. At this point we can conclude that a straightforward model utilizing known physics input at all stages does a reasonable job in reproducing important characteristics of fission data. We are able to correlate all of the cross sections from previous experiments and our data (except for the $\text{Fe} + \text{Ta}$ reaction where fission becomes a 1% branch and is very sensitive to the detailed parameters in the model) without adjusting parameters.

ACKNOWLEDGEMENTS

Work performed under the auspices of the U. S. Department of Energy by the Lawrence Livermore National Laboratory under contract number W-7405-ENG-48, Los Alamos National Laboratory, Lawrence Berkeley Laboratory and Argonne National Laboratory.

REFERENCES

1. V. E. Viola, Nucl. Phys. A502, 531C (1989).
2. Participants in the experiments at various stages have been:
M. Begemann-Blaich, T. Blaich, M. M. Fowler and J. B. Wilhelmy/Los Alamos National Laboratory, Los Alamos, NM 87545; H. C. Britt, D. J. Fields, L. F. Hansen, R. G. Lanier, D. J. Massoletti, M. M. Namboodiri, B. A. Remington, T. C. Sangster, G. L. Struble and M. L. Webb/Lawrence Livermore National Laboratory, Livermore, CA 94550; Y. D. Chan, A. Dacal, A. Harmon, J. Leyba, J. Pouliot, and R. G. Stokstad/Lawrence Berkeley Laboratory, Berkeley, CA 94720; S. Kaufman and F. Videbaek/Argonne National Laboratory, Argonne, IL 60439; and Z. Fraenkel/Weizmann Institute of Science, 76100 Rehovot, Israel.
3. M. M. Fowler et al., Nucl. Inst. and Methods A281, 517 (1989).
4. M. Begemann-Blaich et al., Phys. Rev. (in preparation).
5. T. Blaich et al., Phys Rev C (in preparation)
6. V. E. Viola et al., Nucl. Phys. A471 (1987) 53c.
7. Y. Yariv et al., Phys. Rev. C20, 2227 (1979).
8. Y. Yariv et al., Phys. Rev. C24, 488 (1981).
9. A. Gavron, Phys. Rev. C21, 230 (1980).
10. A. Gavron et al., Phys. Rev. C35, 579 (1987).
11. P. Grange et al., Phys. Rev. C34, 209 (1986).
12. U. Lynen et al., Nucl. Phys. A378, 129c (1982).
13. F. D. Becchetti et al., Phys. Rev. C28, 276 (1983).
14. D. J. Morrissey et al., Phys. Rev. C 21, 1783 (1980).

FIGURE CAPTIONS

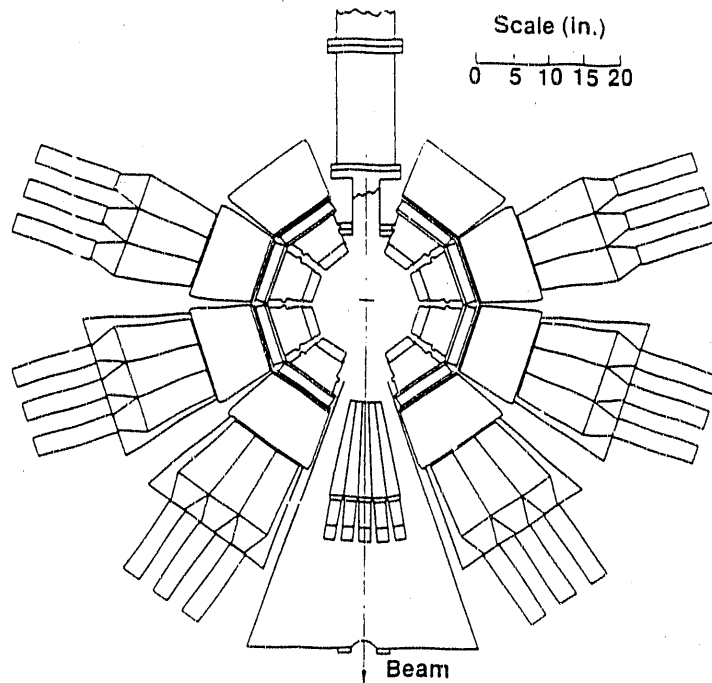
- Fig. 1 Schematic drawing of experimental apparatus.
- Fig. 2 Typical time of flight versus delta E correlation showing separation of different particle types.
- Fig. 3 Correlation of Z_1 vs. Z_2 for binary coincidences for which both fragments were fully identified in the FAGODA. The lowest cut is 6 events per Z-bin; the contour lines indicate increases by factors of two.
- Fig. 4 Mean values for parallel and perpendicular momentum transfer to the fissioning systems studied.
- Fig. 5 Comparison of mean parallel momentum transfer in Fe + Th system to previous results with lighter projectiles [Ref. 6].
- Fig. 6 Comparison of mean folding angles with mean parallel momentum transfer for all systems studied.
- Fig. 7 Results of the intranuclear cascade for Nb + Au at 100 MeV/A. The four parts show (a) excitation energy, (b) parallel momentum, (c) angular momentum, and (d) mass number of the target residues in ten bins of impact parameter. The error bars indicate the widths of the distributions in the respective bins.
- Fig. 8 Correlation between excitation energy and parallel momentum transfer for Nb + Au at 100 MeV/A as predicted by the intranuclear cascade. The error bars indicate the widths of the distributions in the respective bins.

Fig. 9 Comparison of experimental (full circles) and calculated (open circles) parallel momentum transfer distributions for four target projectile combinations to 100 MeV/A: (a) Nb + Au, (b) Fe + Au, (c) Fe + Th, and (d) Fe + Ta. The experimental data have a systematic uncertainty of 10% from uncertainties in the beam flux and target thickness; the statistical errors on these data are small.

Fig. 10 Comparison of experimental (open circles) and calculated (full circles) laboratory scattering angle distributions for the same target-projectile combinations as in Figure 9. The error bars indicate a systematic uncertainty in beam flux and target thickness; the statistical errors on these data are small.

Fig. 11 Comparison of experimental (full circles) and calculated (open circles) charge loss as a function of parallel momentum transfer for Nb + Au at 100 MeV/A. The error bars show the statistical uncertainty of the mean charge loss in the respective bins of parallel momentum transfer.

(A) General Detector Layout



(B) Schematic Diagram of a Pagoda Module

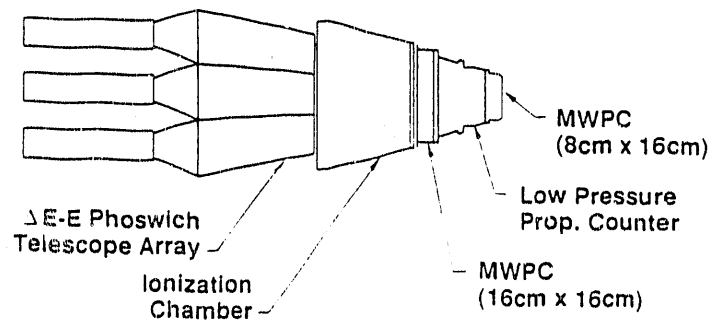


Fig. 1

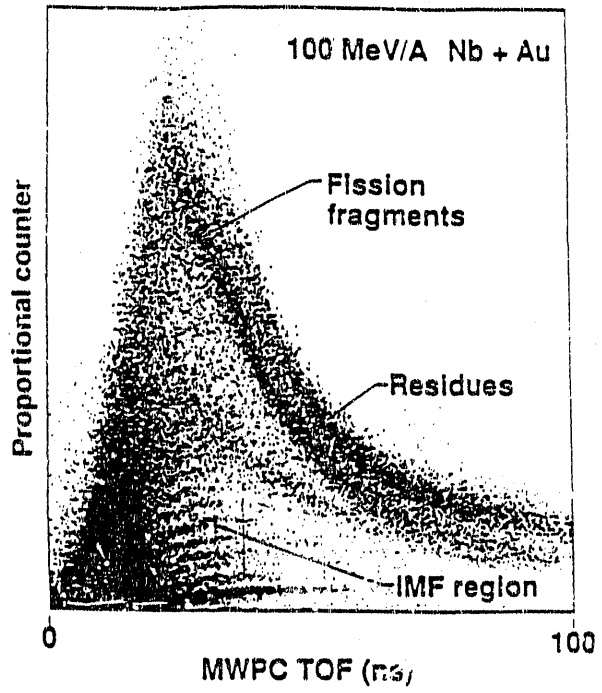


Fig. 2

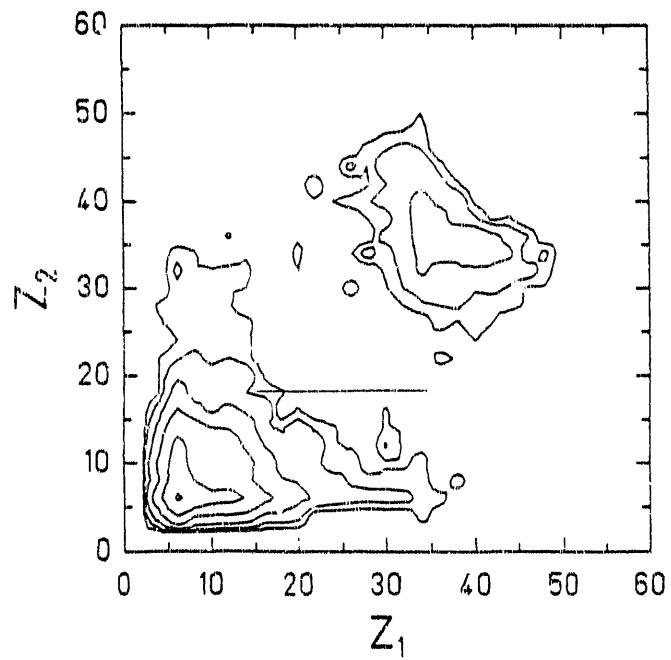


Fig. 3

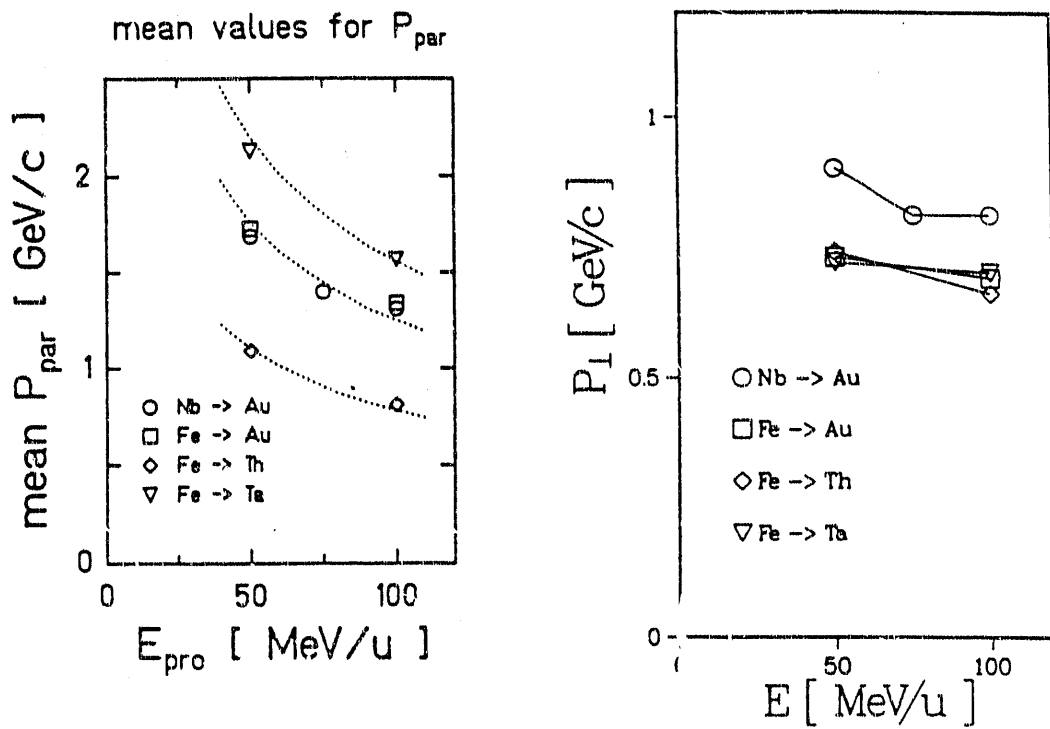


Fig. 4

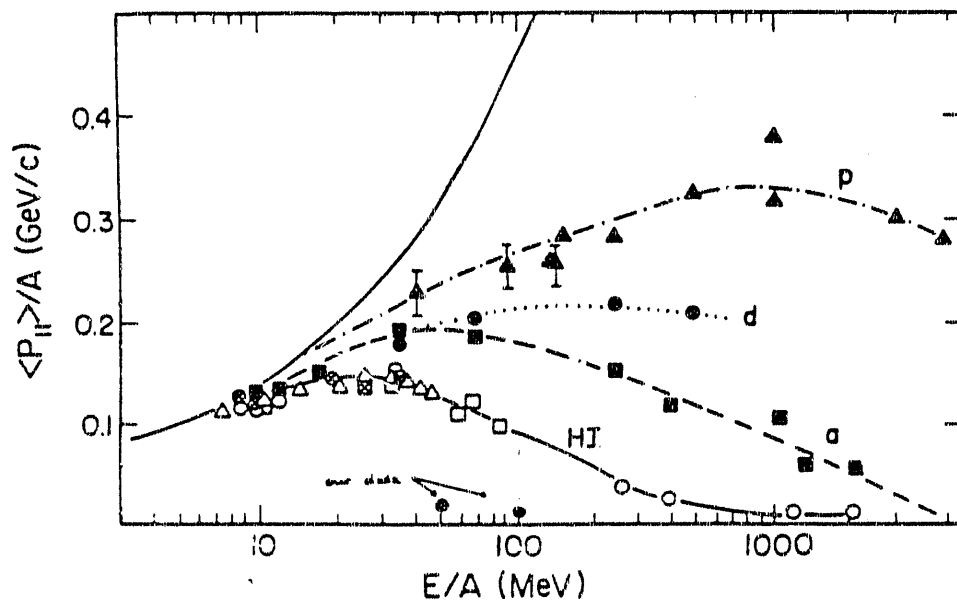


Fig. 5

folding angles for all systems

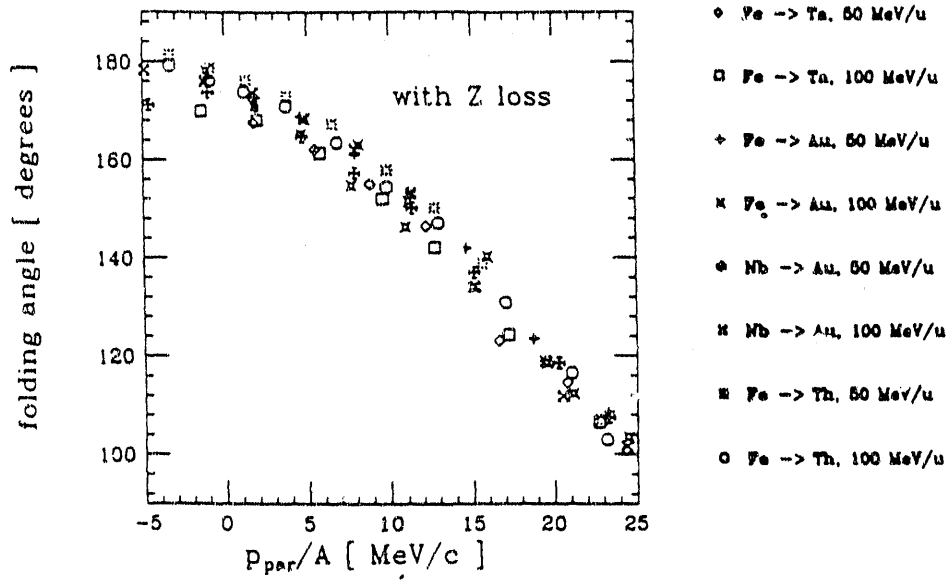


Fig. 6

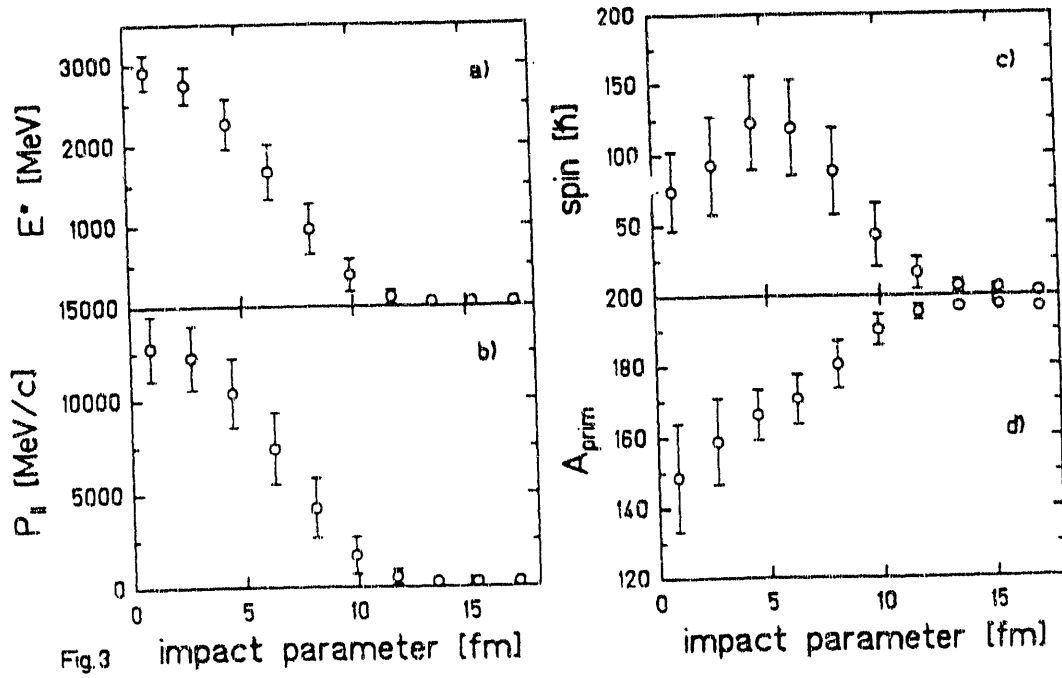


Fig. 7

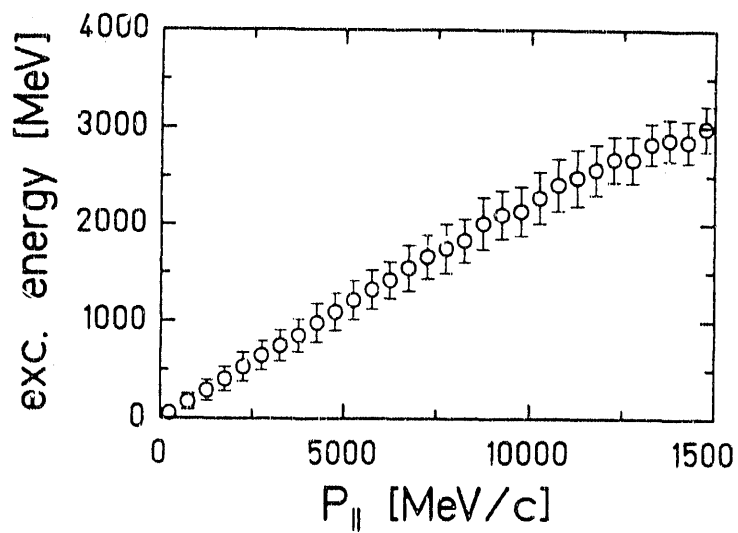


Fig. 8

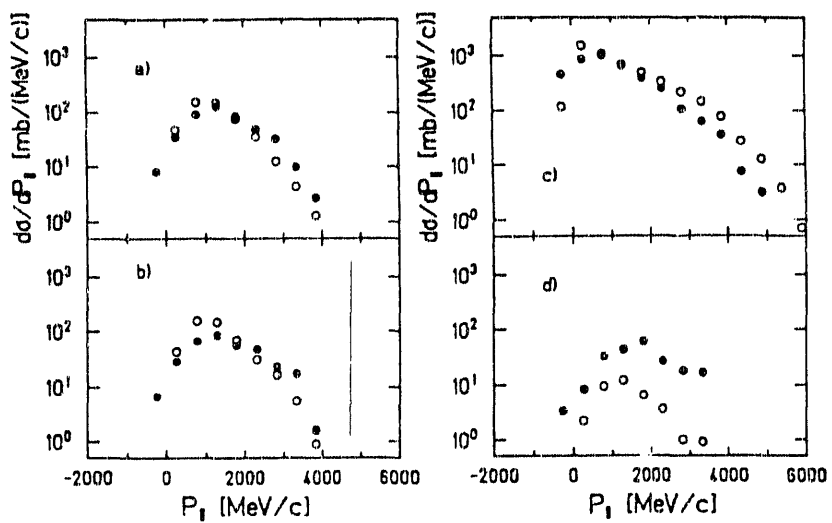


Fig. 9

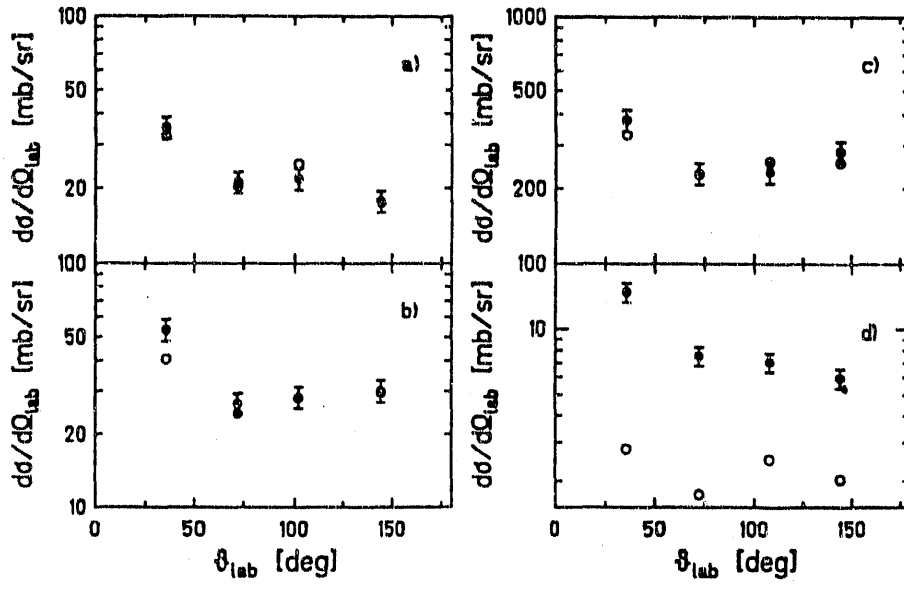


Fig. 10

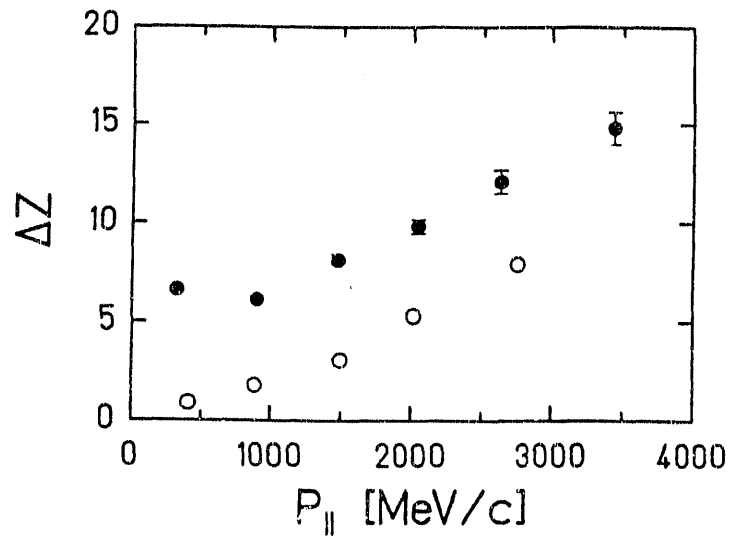


Fig. 11

END

DATE FILMED

02 / 08 / 91

